ISSN 0006-2979, Biochemistry (Moscow), 2011, Vol. 76, No. 6, pp. 694-701. © Pleiades Publishing, Ltd., 2011.
Published in Russian in Biokhimiya, 2011, Vol. 76, No. 6, pp. 849-857.

Purification, Primary Structure, and Properties of *Euphorbia characias* Latex Purple Acid Phosphatase

F. Pintus[#], D. Spano[#], S. Corongiu, G. Floris, and R. Medda*

Department of Applied Sciences in Biosystems, University of Cagliari, Cagliari, Italy;
fax: +39 (070) 675-4523; E-mail: rmedda@unica.it

Received November 25, 2010
Revision received January 22, 2011

Abstract—A purple acid phosphatase was purified to homogeneity from *Euphorbia characias* latex. The native protein has a molecular mass of 130 ± 10 kDa and is formed by two apparently identical subunits, each containing one Fe(III) and one Zn(II) ion. The two subunits are connected by a disulfide bridge. The enzyme has an absorbance maximum at 540 nm, conferring a characteristic purple color due to a charge-transfer transition caused by a tyrosine residue (Tyr172) coordinated to the ferric ion. The cDNA nucleotide sequence contains an open reading frame of 1392 bp, and the deduced sequence of 463 amino acids shares a very high degree of identity (92-99%) to other purple acid phosphatases isolated from several higher plants. The enzyme hydrolyzes well *p*-nitrophenyl phosphate, a typical artificial substrate, and a broad range of natural phosphorylated substrates, such as ATP, ADP, glucose-6-phosphate, and phosphoenolpyruvate. The enzyme displays a pH optimum of 5.75 and is inhibited by molybdate, vanadate, and Zn^{2+}, which are typical acid phosphatase inhibitors.

DOI: 10.1134/S0006297911060101

Key words: acid phosphatase, *Euphorbia characias*, iron ion, metalloenzymes, purple phosphatase, zinc ion

Phosphatases are enzymes usually classified as acid or alkaline depending on their pH optimum for catalytic activity being below or above pH 7. Acid phosphatases (APs; EC 3.1.3.2) are ubiquitous enzymes ranging from microorganisms (fungi and bacteria) to plants and animals [1, 2]. APs catalyze the hydrolysis of phosphate monoesters, and their function seems to be the release, transport, and recycling of P_i, a crucial macronutrient for cellular metabolism and bioenergetics. Plant APs have been isolated and characterized from several sources [2], and some of these have been crystallized [3, 4]. These enzymes, homodimeric or heterodimeric glycoproteins, can be intracellular (localized in cytoplasm and vacuole) or extracellular (localized in cell wall) [5].

Purple acid phosphatases (PAPs) represent a distinct class of acid phosphatases. Their typical absorbance spectrum with maximum at 530-560 nm, with a characteristic purple color, is due to a charge-transfer transition between a tyrosine residue and a coordinated ferric iron [4]. These enzymes contain a Fe(III)-Me(II) metal center, where Me(II) can be Zn, Mn, or Fe ([6, 7] and references therein). Purple acid phosphatases from bacteria, mammals, and plants contain seven highly conserved metal ligand residues (**D**XG-G**D**XX**Y**-GN**H**(D/E)-VXX**H**-G**H**X**H**; bold letters indicate metal ligand residues, dashes indicate separation between blocks) forming dimetallic active centers. Moreover, the structure of the catalytic site and other domains of purple acid phosphatase are also highly conserved [8]. Plants contain two major groups of PAPs: small PAPs, 35-40 kDa monomeric proteins homologous to mammalian enzymes, and large PAPs, 110-130 kDa homodimeric proteins, with or without a disulfide bridge between the two subunits [9].

A large number of plant species exude a milky, variously colored sap known as latex. Contained in laticifers, specialized cells forming vessel-like structures, plant latex is a complex environment with a diversified composition that includes terpenoid compounds, alkaloids, and a number of proteins. Several proteins had been well characterized in the latex of the Mediterranean shrub *Euphorbia characias* and, very recently, a soluble metallo-

Abbreviations: AP, acid phosphatases; ELPAP, *Euphorbia* latex purple acid phosphatase (protein); PAPs, purple acid phosphatases; *p*-NPP, 4-nitrophenyl phosphate; RT-PCR, reverse transcription-polymerase chain reaction; SDS-PAGE, sodium dodecyl sulfate polyacrylamide gel electrophoresis.

[#] These authors contributed equally to this work.

* To whom correspondence should be addressed.

protein nucleotide pyrophosphatase/phosphodiesterase, containing one Ca(II) and one Mg(II) ion, was purified to homogeneity from it ([10] and references therein).

In this paper we describe the purification and some biochemical characteristics of a purple acid phosphatase (ELPAP) extracted from *E. characias* latex. The substrate specificity, effect of inhibitors, activation energy, pH effect, and other biochemical characteristics of the enzyme have been investigated. Moreover, we isolated and sequenced the cDNA encoding ELPAP, and here we report the nucleotide and the deduced amino acid sequences showing the conserved residues involved in several domains. This study leads us to learn more about the biochemistry of the proteins of *Euphorbia* latex and to hypothesize a possible physiological role of the joined action of two secreted metalloproteins.

MATERIALS AND METHODS

ATP, ADP, AMP, GMP, 4-nitrophenyl phosphate (*p*-NPP), glucose-1-phosphate, glucose-6-phosphate, inositol-1-phosphate, phosphoenolpyruvate, pyridoxal-5-phosphate, 2,3-bisphosphoglycerate, iron chloride, calcium chloride, magnesium chloride, manganese chloride, copper chloride, zinc chloride, nickel chloride, cobalt chloride, cadmium chloride, sodium fluoride, sodium molybdate, and sodium vanadate, tartrate, citrate, and EDTA were from Sigma Chemical Co (USA).

Euphorbia characias latex, drawn from cut branches, was collected at several locations in southern Sardinia (Italy), immediately frozen at −80°C, lyophilized, and stored at −20°C until use.

Enzyme purification. ELPAP was purified from the lyophilized *E. characias* latex by the following steps at 4°C unless otherwise indicated.

Step 1. Acetone powder. The lyophilized material was poured into 1 liter of cold acetone and kept for 45 min with constant stirring at –20°C. The acetone powder was collected by filtration on a Buchner funnel. Acetone powder (30 g) was mixed with 700 ml H_2O with continuous stirring for 2 h and centrifuged at 14,300*g* for 45 min.

Step 2. Ammonium sulfate fractionation. The supernatant was made 25% saturated with ammonium sulfate with constant stirring for 30 min and centrifuged at 14,300*g* for 30 min. The precipitate was discarded, and the supernatant was brought to 80% saturation with ammonium sulfate with constant stirring for 30 min and centrifuged at 14,300*g* for 30 min. The pellet was dissolved in 40 ml of 10 mM Tris-HCl buffer, pH 7.0, and dialyzed for 12 h against the same buffer.

Step 3. DEAE-cellulose chromatography. The dialyzed protein was loaded onto a DEAE-cellulose column (2.8 × 14 cm) equilibrated and washed with 10 mM Tris-HCl buffer, pH 7.0. The enzyme was then eluted with 100 mM Tris-HCl buffer, pH 7.0. The fractions with the same specific activity were pooled and concentrated by ultrafiltration.

Step 4. Gel-filtration chromatography. The concentrated solution was loaded onto a column (2 × 100 cm) of Sephacryl S-200 (fine grade) equilibrated and eluted at 4°C with 100 mM Tris-HCl buffer, pH 7.5, containing 300 mM NaCl. The fractions with the highest specific activity were pooled and concentrated by ultrafiltration.

Analytical polyacrylamide gel electrophoresis (PAGE). Electrophoresis in nondenaturing conditions was performed as previously described [11]. The protein band with ELPAP activity was detected after the electrophoretic run by staining the gel in 100 mM Na-acetate buffer, pH 5.75, containing 1 mM *p*-NPP.

SDS-PAGE was carried out according to Weber and Osborne [12]. The protein samples for SDS-PAGE were heated at 100°C for 5 min in 10 mM Tris-HCl buffer, pH 7.0, containing 1% SDS in the presence and in the absence of 100 mM 2-mercaptoethanol. For molecular mass determination, the standards used were: myosin (200 kDa), β-galactosidase (116.2 kDa), phosphorylase *b* (97.4 kDa), bovine serum albumin (66.2 kDa), ovalbumin (45 kDa), glyceraldehydes-3-phosphate dehydrogenase (36 kDa), carbonic anhydrase (29 kDa), and α-lactalbumin (14.2 kDa).

Deglycosylation analysis. Protein samples were denatured by boiling for 5 min and then deglycosylated with N-glycosidase (5 mg/ml) in 50 mM Na-P_i buffer, pH 7.2, at 37°C for 12 h. Controls were performed in samples without N-glycosidase. Protein samples were analyzed by SDS-PAGE.

Gel filtration and molecular mass determination. The M_r under nondenaturing conditions was estimated by gel filtration using a column (2 × 100 cm) of Sephacryl S-200 (fine grade) equilibrated and eluted at 4°C with 100 mM Tris-HCl buffer, pH 7.5, containing 300 mM NaCl. The distribution coefficient K_d was obtained as described [13] using blue dextran to measure the void volume V_o and tyrosine to measure the total volume (V_i). The standards used were: β-amylase (200 kDa), alcohol dehydrogenase (150 kDa), bovine serum albumin (66 kDa), carbonic anhydrase (31 kDa), and cytochrome *c* (12.4 kDa).

Metal content. The amounts of Fe^{3+}, Mn^{2+}, and Zn^{2+} were measured by atomic absorption using an IRIS Intrepid Spectrometer (Thermo Elemental, USA). The spectral lines chosen were 248.300 nm for Fe^{3+}, 259.373 nm for Mn^{2+}, and 206.200 nm for Zn^{2+}.

Protein determination. Protein concentration was measured by the Bradford method [14] using bovine serum albumin as a standard for the calibration curve.

Spectroscopic features. Spectrophotometric determinations were recorded with an Ultrospec 2100 spectrophotometer (Biochrom Ltd, UK).

Enzyme assays using *p*-NPP as substrate. For routine measurements of ELPAP activity, the hydrolysis of *p*-NPP was determined by direct spectrophotometric meas-

urement of the increase in absorbance at 405 nm resulting from the release of 4-nitrophenolate (ε_{405} = 3880 $M^{-1}\cdot cm^{-1}$). The reaction mixture contained 100 mM Na-acetate buffer, pH 5.75 (the pH value at which the enzyme showed the best activity toward this substrate; see section "Analytical polyacrylamide gel electrophoresis (PAGE)"), 5 mM *p*-NPP, and enzyme in a total volume of 1 ml. In experiments performed at different pH values, due to the variable ionization state of the 4-nitrophenol/4-nitrophenolate, the molar absorption was measured at 405 nm at each pH used and normalized to that at pH 5.75.

The K_m value for *p*-NPP was estimated by nonlinear regression analysis from the Michaelis–Menten equation from data measured in 100 mM Na-acetate buffer, pH 5.75. Catalytic center activity (k_{cat}) was defined as (mole of substrate consumed)/(mole of enzyme monomer) × sec^{-1}. All kinetic parameters are the means of three determinations.

Analysis of phosphate released from different substrates. When phosphorylated substrates were used, the inorganic phosphate released in the reaction was estimated using a malachite green assay kit (SensoLyte™ MG Phosphate Assay Kit; AnaSpec, USA). ELPAP activity was measured after incubation in the presence of each of various substrates at 25°C for 2 h. The assays were quenched with malachite green reagent, and the absorbance values at 630 nm were measured after incubation for 20 min at room temperature. The amount of P_i released (μmoles) was calculated with a standard curve determined for inorganic phosphate according to the manufacturer's recommendations. Controls were run for background amounts of P_i present at each substrate concentration tested.

Isolation of RNA and RT-PCR. For total RNA extraction from laticifers, *E. characias* branches were sliced, and the fresh latex (~5 ml) flowed directly into a tube containing 20 ml of 2× RNA extraction buffer (0.1 M Tris-HCl, 0.3 M LiCl, 0.01 M EDTA, 10% SDS, pH 9.5) with 5 ml of RNAlater solution (Sigma) to stabilize and protect RNA. The latex solution was mixed and centrifuged at 8000*g* for 15 min at 20°C. The supernatant fraction was processed using TRI Reagent RNA isolation reagent (Sigma) according to the manufacturer's instructions. The quality of purified RNA was verified by gel electrophoresis using 1% denaturing agarose gel stained with ethidium bromide and by the absorption spectrum from 220 to 300 nm. To obtain the cDNA, *Euphorbia* RNA was reverse transcribed with an oligo-dT primer using an enhanced avian myeloblastosis virus reverse transcriptase enzyme (Sigma).

***Euphorbia* acid phosphatase cDNA-amplification by PCR with hybrid primers.** Degenerate oligonucleotide primers were designed using the consensus degenerate hybrid oligonucleotide primer (CODEHOP) strategy [15] starting from the alignment of multiple purple acid phosphatase protein sequences from different plant sources. Five sequences were chosen from the GenBank database and aligned using ClustalW (http://www.ebi.ac.uk/clustalw) and then cut into blocks using Block Marker software (http://blocks.fhcrc.org/blocks/). Primers were designed using the default parameters at the CODEHOP server (http://blocks.fhcrc.org/codehop.html), and sets of sense and antisense primers were selected for the protein. For *Euphorbia* purple acid phosphatase cDNA the sense primers 5′-CTACAACGCCCCTCAGcargtncayat-3′ and 5′-TGTTCGTGGGCGACCTGwsntaygcnga-3′ were used in association with the antisense primers 5′-TGTCGGCGTAGGACAGGtcnccnavraa-3′ and 5′-GGGGACGTGCATCAGCacdatnarcca-3′, respectively. Each primer presents the consensus clamp given in upper case, whereas the degenerate core is in lower case: y = [C, T]; r = [A, G], w = [A, T], s = [C, G], and n = [A, G, C, T].

PCR was performed in a solution containing 1.5 mM $MgCl_2$, 100 mM Tris-HCl, pH 8.3, 50 mM KCl, 200 μM of dNTP mix, 1 μM sense primer, 1 μM antisense primer, 1 μg of *Euphorbia* cDNA, and 1-3 units of *Taq* DNA polymerase (Sigma). Thermal cycles of amplification were carried out in a Personal Eppendorf Mastercycler (Eppendorf, Germany).

Rapid amplification of cDNA ends (RACE). Rapid amplification of the 5′ and 3′ ends was done as reported [16] using antisense-specific primers and the anchor primer provided in the RACE kit (Roche Diagnostics, Germany). To perform 5′ RACE for *Euphorbia* purple acid phosphatase cDNA, the antisense-specific primer 5′-GCTATGCTCTAACTTTCTAATGGTACA-3′ was used in a reverse transcription reaction with 2 μg of *E. characias* total RNA. The first-strand cDNA was purified from unincorporated nucleotides and primers using a High Pure PCR Purification Kit (Roche Diagnostics). A homopolymeric tail was added to the 3′ end of RT-PCR products, and the obtained cDNA was amplified by PCR using the nested antisense-specific primer 5′-AAC-CTTCTTTTTTGTGGTATTTTCAGG-3′ and the oligo dT-anchor primer provided in the RACE kit according to the protocol supplied. For 3′ RACE, the first strand cDNA was obtained using the oligo dT-anchor primer and amplified using the sense-specific primer 5′-GCCGGCCAT-GTTCATGCTTATGAAAGA-3′ or 5′-TCAGCTCCCG-TTTATATTACCATTGGG-3′ and the antisense PCR anchor primer provided in the RACE kit. PCR reactions were performed using 1-3 units of *Taq* DNA polymerase (Sigma) under different experimental conditions.

cDNA sequencing and analysis. cDNA was sequenced by BMR Genomics (Italy). Nucleotide and deduced amino acid sequence analyses were performed with programs accessible on the internet. Nucleotide sequences were translated using the ExPASy translate routine software (http://ca.expasy.org/). Similarities were analyzed with the advanced BLAST algorithm available at

the National Center for Biotechnology Information website (http://www.ncbi.nlm.nih.gov/) and with the FASTA algorithm version 3.0 from the European Bioinformatics Institute website (http://www.ebi.ac.uk/fasta33/index.htlm). Sequences were aligned with ClustalW.

RESULTS AND DISCUSSION

Enzyme purification, criteria of purity, carbohydrate content, and relative molecular mass determination. Table 1 presents a summary of the purification procedure for ELPAP. The enzyme was purified 83-fold with a yield of about 14%. The Sephacryl S-200 chromatography purification step effectively served to remove a significant amount of contaminating proteins. A single chromatographic peak of phosphatase activity was observed, and ELPAP was eluted from the Sephacryl column with a K_d of 0.26, corresponding to a protein of a molecular mass of 130 ± 10 kDa.

ELPAP obtained by the reported purification procedure was tested for homogeneity by PAGE under different conditions. One protein band was present on PAGE under nondenaturing conditions with Coomassie Blue staining, and one protein band in the same position showed enzymatic activity by staining with *p*-NPP (not shown). When analyzed by SDS-PAGE in the presence of mercaptoethanol, ELPAP migrated as a single polypeptide chain of 68 ± 4 kDa (Fig. 1a). The same analysis performed in the absence of mercaptoethanol revealed that ELPAP migrated as a dimer with a molecular mass of 130 ± 10 kDa (Fig. 1b). All data reported suggest that the native enzyme has a homodimeric structure, and the presence of a disulfide bond linking the two subunits of the protein could be hypothesized. We analyzed the extent of glycosylation of ELPAP by treating denatured protein samples with N-glycosidase. Comparing the SDS-PAGE mobility with that of untreated controls, a

Table 1. Purification of *Euphorbia* latex acid phosphatase

Step	Total protein, mg	Specific activity, unit/mg	Yield, %
Acetone powder crude extract	1300	7.2	100
Ammonium sulfate fractionation	200	18.5	39.4
DEAE-cellulose chromatography	38	54.8	22
Gel-filtration chromatography (S-200)	2.2	598	14

Note: Starting material was 150 ml latex. Units were calculated as μmol/min.

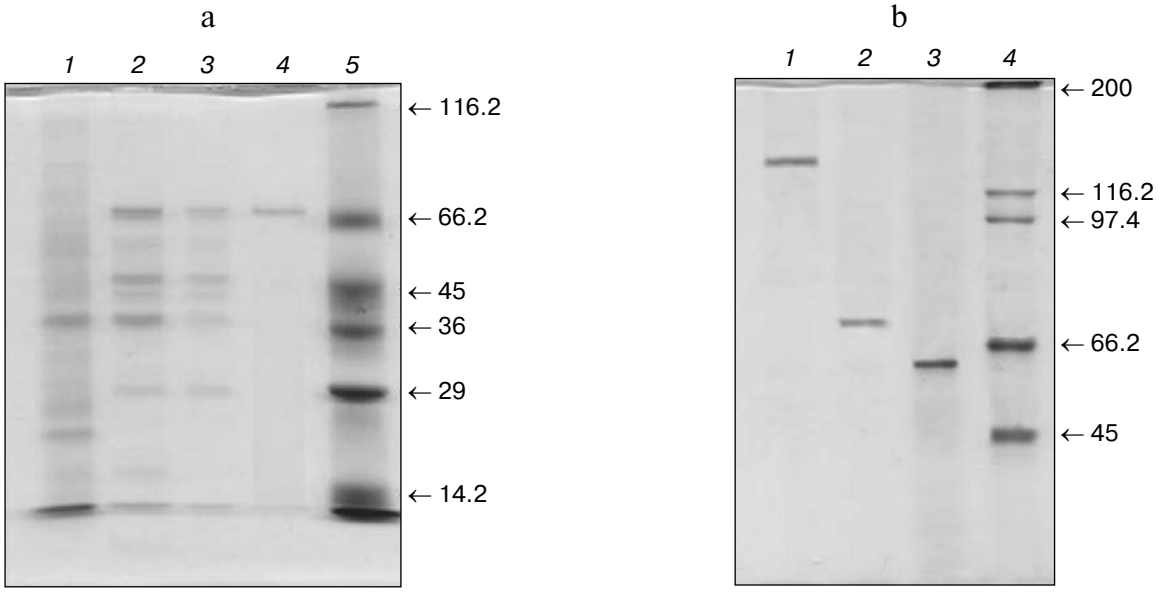

Fig. 1. ELPAP molecular mass determination by SDS-PAGE. a) Protein samples after the purification steps of ELPAP: *1*) acetone powder crude extract (2 μg); *2*) ammonium sulfate fractionation (0.6 μg); *3*) DEAE-cellulose chromatography (0.4 μg); *4*) gel chromatography on Sephacryl S-200 (0.3 μg); *5*) standard proteins: β-galactosidase (116.2 kDa), bovine serum albumin (66.2 kDa), ovalbumin (45 kDa), glyceraldehydes-3-phosphate dehydrogenase (36 kDa), carbonic anhydrase (29 kDa), and α-lactalbumin (14.2 kDa). b) Purified enzyme: *1*) 0.3 μg purified ELPAP in the absence of mercaptoethanol; *2*) 0.3 μg purified ELPAP in the presence of mercaptoethanol; *3*) 0.4 μg deglycosylated ELPAP; *4*) standard proteins: myosin (200 kDa), β-galactosidase (116.2 kDa), phosphorylase *b* (97.4 kDa), serum albumin (66.2 kDa), ovalbumin (45 kDa).

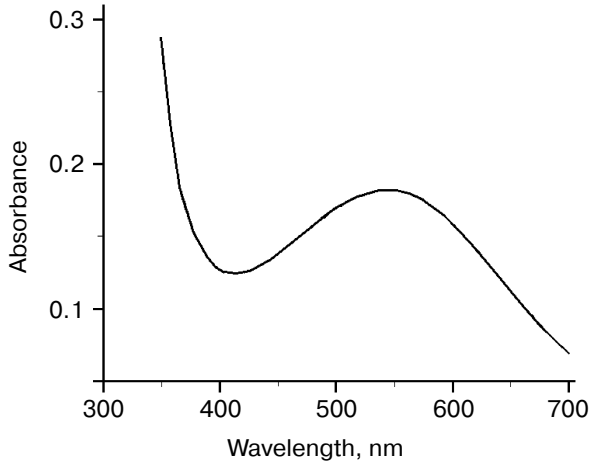

Fig. 2. Visible absorption spectrum of *Euphorbia* purple acid phosphatase. The spectrum was obtained using ELPAP (62 μM) in 100 mM Tris-HCl, pH 7.0.

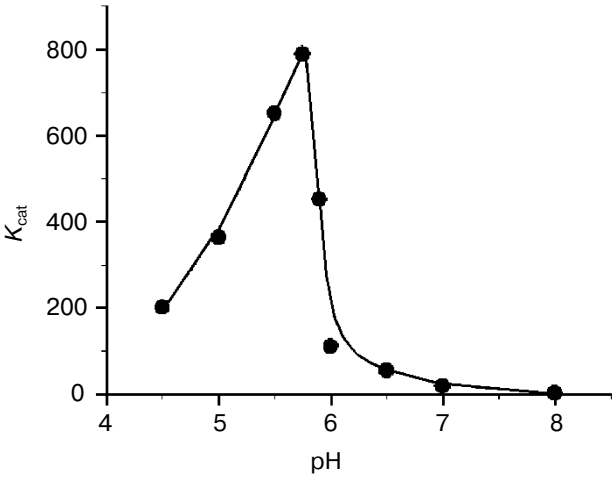

Fig. 3. Effect of pH on ELPAP activity using *p*-NPP as substrate. Buffers used (100 mM) were: Na-acetate (pH 4.5-6.0), Bis/Tris-HCl (pH 6.0-7.0), and Tris-HCl (pH 7.0-8.0). ELPAP, 16 nM; *p*-NPP, 5 mM.

significant shift in molecular mass from 68 ± 4 to 58 ± 3 kDa was revealed (Fig. 1b), suggesting that the protein may contain about 12-15% carbohydrates.

Metal determination. Using atomic absorption spectrometry, the analysis of five different samples of purified ELPAP revealed that the enzyme contained a mean of 0.0941% of Fe and 0.116% of Zn. On this basis, a minimum molecular mass of 59.3 and 56.4 kDa can be calculated, respectively. Thus, ELPAP contains 1 mole of Fe and 1 mole of Zn per mole of subunit, while it does not contain Mn.

Absorption spectrum. In addition to the protein absorption maximum at 278 nm, the enzyme showed a maximum at 540 nm in the visible region and had a characteristic purple color. This color, as reported for other PAPs, is due to a charge-transfer transition caused by a tyrosine residue (Tyr172) coordinated to the ferric ion (Fig. 2). The ε_{540} was calculated to be 2900 $M^{-1}\cdot cm^{-1}$.

Effect of pH and temperature on enzyme activity. The pH effect on ELPAP activity was tested in the pH range 4.5-8.0. The buffers used were Na-acetate (pH 4.5-6.0), Bis/Tris-HCl (pH 6.0-7.0), and Tris-HCl (pH 7.0-8.0). For all of the pH values considered, each buffer was used at different concentrations ranging from 10 to 100 mM, and no ionic strength effects were observed for any of the buffers used. The pH dependence of k_{cat} values for *p*-NPP is plotted in Fig. 3. ELPAP showed the highest k_{cat} value of 790 sec^{-1} at pH 5.75. At pH 5.75, the K_m value for *p*-NPP was 0.51 mM. The reaction was first order in enzyme concentration ranging from 10 nM to 1 μM.

The effect of temperature on ELPAP activity was measured in the range of 20-70°C using Na-acetate buffer, pH 5.75, 3.3 nM ELPAP, and *p*-NPP as substrate. The Arrhenius plot was a straight line, yielding an activation energy of 13 kcal/mol. To examine the thermal stability of ELPAP, the enzymatic activity was measured at 25°C, according to the standard assay, after incubation for 30 min in the temperature range reported above. ELPAP was stable at 50°C but lost 70% of its activity at 60°C.

Substrate specificity. The purified enzyme was tested for its activity against a variety of phosphorylated substrates (Table 2). The assay was performed by incubating the native enzyme at 25°C for 2 h in a reaction mixture containing 5 mM substrate and 100 mM Na-acetate buffer, pH 5.75. The released inorganic phosphate was determined as described (see "Materials and Methods", section "Analysis of phosphate released from different

Table 2. Substrate hydrolysis (%) catalyzed by *Euphorbia* purple acid phosphatase

Substrate	Hydrolysis, %
p-NPP	100 ± 4
ATP	100 ± 9
ADP	100 ± 7
AMP	16 ± 2
GMP	66 ± 6
Inositol-1-phosphate	60 ± 8
Glucose-1-phosphate	25 ± 6
Glucose-6-phosphate	104 ± 16
Phosphoenolpyruvate	96 ± 6
2,3-Bisphosphoglycerate	85 ± 6
Pyridoxal-5-phosphate	80 ± 2

Note: Substrate, 5 mM; ELPAP, 100 nM; 100 mM Na-acetate buffer, pH 5.75, 2 h incubation time.

substrates"). AMP was a very poor substrate for ELPAP, and GMP was hydrolyzed better than AMP. The enzyme efficiently hydrolyzed glucose-6-phosphate, phosphoenolpyruvate, 2,3-bisphosphoglycerate, and pyridoxal-5-phosphate and poorly hydrolyzed glucose-1-phosphate and inositol-1-phosphate.

Inhibitors and effectors. ELPAP was inhibited by Zn^{2+}, and the inhibition was shown to be noncompetitive with respect to substrate with a K_i of 70 μM (not shown), whereas other divalent cations (Cd^{2+}, Cu^{2+}, Mn^{2+}, Ni^{2+}, Co^{2+}, Ca^{2+}, Mg^{2+}, Fe^{2+}) did not influence ELPAP activity. Metal chelators EDTA, tartrate, citrate, and fluoride had no inhibitory effect. ELPAP activity was blocked by vanadate and molybdate, which are typical inhibitors of acid phosphatases. The inhibition was shown to be competitive with respect to substrate, and the ELPAP activity was fully restored after dialysis against 100 mM Tris-HCl, pH 7.5, or filtration through a Sephacryl S-200 column. K_i values of 0.1 and 0.8 μM were calculated for vanadate and molybdate, respectively (not shown).

Acid phosphatase cDNA. We cloned the cDNA encoding *Euphorbia* latex AP by RT-PCR. The acid phosphatase cDNA sequence was determined for both strands using a progressive primer design strategy. The *Euphorbia* purple acid phosphatase cDNA contained an open reading frame (ORF) of 1392 bp that extended from the ATG codon at positions 1-3 to the termination codon TAA at position 1392 (Fig. 4), encoding a protein of 463 amino acids. The N-terminal residue of the isolated protein was identified as glycine in the amino acid sequence GKTSVYVR. The cDNA sequence revealed that the glycine residue did not initiate the ORF, but it followed a 22 a.a. leader sequence with characteristics of a secretion signal peptide (Fig. 4). The ELPAP amino acid sequence showed a very high degree of identity (92-99%) to APs isolated from several other higher plants, including *Ricinus communis*, *Ipomoea batatas*, *Populus trichocarpa*, *Medicago truncatula*, *Nicotiana tabacum*, and *Phaseolus vulgaris*.

"Large" PAPs contain characteristic sets of conserved motifs, seven amino acid residues involved in metal binding, and two histidine residues at the site active interacting with the phosphate group of the substrate. These enzymes can be divided into two subfamilies: the first subfamily has only one cysteine residue near position 100, which does not form a linkage between the two subunits of the protein; the second subfamily contains a characteristic cysteine residue near position 340-370, as well as other cysteine residues able to form a disulfide bridge between the subunits. The ELPAP sequence showed two characteristic cysteine residues (Cys95 and Cys350) (see Table 3 and Fig. 4), and a non-conserved cysteine residue at position 24. Moreover, analysis by SDS-PAGE, both in the absence and in the presence of mercaptoethanol, showed that ELPAP migrated as dimer or as monomer, respectively (Fig. 1b). Thus, by analogy with other PAPs, we can include ELPAP in the second subfamily with Cys350 able to form a disulfide bond.

ELPAP is a glycoprotein containing about 12-15% carbohydrates. Submission of the ELPAP sequence to the NetNGlyc 1.0 server (http://www.cbs.dtu.dk/services/NetNGlyc/) permitted the identification of five potential N-glycosylation sites (N-X-S/T) at amino acids 68-70 (NTT), 114-116 (NTT), 148-150 (NRT), 279-281 (NRT), and 376-378 (NMT) (Fig. 4). The ELPAP

Table 3. Conserved cysteine and metal-binding amino acid residues of ELPAP compared with other "large" plant PAPs

Source of PAP and EMBL accession number[a]	Cysteine near position 100[b]	Cysteine near position 350[b]	Metal-binding amino acid residues
*Lupinus luteus** AJ458943	GYVHH**C**	SGHRFPI	G**D**LG G**D**LS**Y**G**N**HE VLM**H** G**H**V**H**
*Arabidopsis thaliana** AY050812	GFIHH**C**	SGDRYPV	G**D**MG G**D**LS**Y**G**N**HE VLM**H** G**H**V**H**
*Oryza sativa** AF356352	GYIHH**C**	SGNRYPV	G**D**LF G**D**LS**Y**G**N**HE VLM**H** G**H**V**H**
*Allium cepa** AB052619	GYIHH**C**	SGNRYPI	G**D**LG G**D**LS**Y**G**N**HE VLM**H** G**H**V**H**
*Glycine max** AY151271	GYIHH**C**	GGNRYPL	G**D**LG G**D**LS**Y**G**N**HE VLM**H** G**H**V**H**
Ipomea batatas AJ006224	GYIHH**C**	NGE**C**TPV	G**D**LG G**D**LS**Y**G**N**HE VLM**H** G**H**V**H**
Ipomea batatas AF200826	GYIHH**C**	NGK**C**TPV	S**D**IG G**D**SL**Y**G**N**HE VLM**H** G**H**V**H**
Ipomea batatas AF200825	AFIHH**C**	NAK**C**TPV	G**D**LG G**D**LS**Y**G**N**HE VLV**H** G**H**V**H**
Glycine max AF200824	GFIHHT	NGL**C**APV	G**D**LG G**D**LS**Y**G**N**HE VLM**H** G**H**V**H**
Arabidopsis thaliana Q38924	GFIHH**C**	NGL**C**EPI	G**D**LG G**D**LS**Y**G**N**HE VLV**H** G**H**V**H**
Phaseolus vulgaris AJ001270	GFIHHT	NGL**C**TPV	G**D**LG G**D**LS**Y**G**N**HE VLM**H** G**H**V**H**
Euphorbia characias HM641814	GFIYY**C**	NGE**C**TPV	G**D**LG G**D**LS**Y**G**N**HE ILM**H** G**H**V**H**

[a] Reference [8].
[b] Position of cysteine residues in mature protein.
* "Large" PAP subfamily (not containing a disulfide bridge between the two subunits).

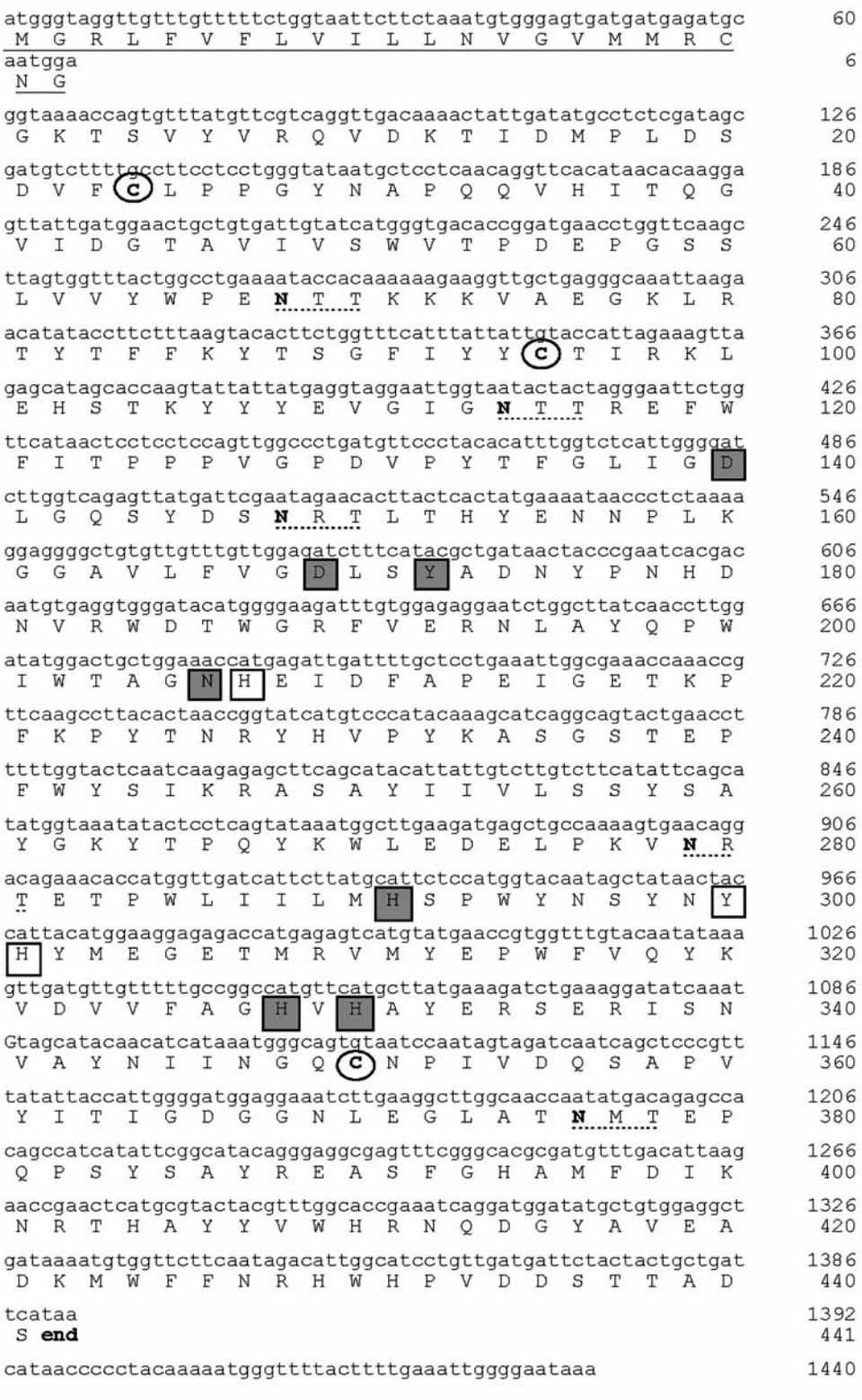

Fig. 4. Nucleotide and deduced amino acid sequences of *Euphorbia characias* purple acid phosphatase. The nucleotide sequence is numbered in the 5′ to 3′ direction. The terminal taa codon is indicated by the end. The signal peptide portion of the protein is underlined. G corresponds to the N-terminal residue in mature ELPAP. The potential N-glycosylation sites are underlined with a dotted line. His207, His301, and Tyr300 interacting with the substrate during catalytic activity are boxed. Metal-binding amino acids (Asp140, Asp169, Tyr172, Asn206, His291, His328, His330) are in gray boxes. Cys24, Cys95, and Cys350 are circled.

sequence harbors all highly conserved amino acid residues of plant PAPs that are coordinated to metal ions (Table 3).

Acid phosphatases are ubiquitous enzymes present in various organs of germinating seeds and in different cell compartments. The wide distribution of APs suggests that they could be of great importance, although the physiological function(s) and metabolic control of these enzymes is not yet fully understood. The major metabolic function of these enzymes seems to be in the release, transport, and recycling of phosphate (P_i), a crucial macronutrient for cellular metabolism and bioenergetics. Phosphate availability is an important factor in regulating growth and development of plants. However, plants often grow in P_i deficiency and adopt metabolic adaptations aimed to increase the acquisition of P_i, promoting their growth and survival. Intracellular APs are believed to remobilize and scavenge P_i from intracellular phosphate monoesters and anhydrides in P_i-deficient plants, whereas secreted APs are probably involved in P_i scavenging from extracellular organic phosphate monoesters [17].

The data presented in this work show that a secreted purple acid phosphatase is present in the latex of the shrub *Euphorbia characias*. Moreover, very recently a nucleotide pyrophosphatase/phosphodiesterase was isolated and characterized from *Euphorbia* latex. Therefore, the contemporary presence of a pyrophosphatase/phosphodiesterase and a purple acid phosphatase in *Euphorbia* latex take us to hypothesize a single or a joined participation of these important enzymes in the metabolism of nucleotides. Thus *Euphorbia* phosphodiesterase can produce phosphomonoesters from diesters of phosphoric acid, and these monoesters can be well hydrolyzed by ELPAP. Moreover, the ELPAP activity toward glucose-6-phosphate, phosphoenolpyruvate, bisphosphoglycerate, and pyridoxal-5-phosphate could ensure an adequate P_i supplement in this shrub.

In conclusion, an emerging scenario suggests that the role played by latex in plants might be significantly less passive than previously believed.

Nucleotide sequence data are available in the GenBank database under accession number HM641814.

This study was partially supported by a grant from "Fondazione Banco di Sardegna" (Sassari, Italy) and from Regione Autonoma della Sardegna, Progetti di Ricerca di Base CRP2-22.

REFERENCES

1. Klabunde, T., Strater, N., Krebs, B., and Witzel, H. (1995) *FEBS Lett.*, **367**, 56-60.
2. Hoehamer, C. F., Mazur, C. S., and Wolfe, N. L. (2005) *J. Agric. Food Chem.*, **53**, 90-97.
3. Strater, N., Frohlich, R., Schiemann, A., Krebs, B., Korner, M., Suerbaum, H., and Witzel, H. (1992) *J. Mol. Biol.*, **224**, 511-513.
4. Klabunde, T., Strater, N., Frohlich, R., Witzel, H., and Krebs, B. (1996) *J. Mol. Biol.*, **259**, 737-748.
5. Ehsanpour, A. A., and Amini, F. (2003) *Afr. J. Biotechnol.*, **5**, 133-135.
6. Wilcox, D. E. (1996) *Chem. Rev.*, **96**, 2435-2458.
7. Olczak, M., Ciuraszkiewicz, J., Wojtowicz, H., Maszczak, D., and Olczak, T. (2009) *FEBS Lett.*, **583**, 3280-3284.
8. Olczak, M., and Watorek, W. (2003) *Physiol. Plant.*, **118**, 491-498.
9. Olczak, M., Morawiecka, B., and Watorek, W. (2003) *Acta Biochim. Pol.*, **50**, 1245-1256.
10. Pintus, F., Spano, D., Bellelli, A., Angelucci, F., Floris, G., and Medda, R. (2009) *Plant Sci.*, **177**, 636-642.
11. Gabriel, O. (1971) in *Methods in Enzymology* (Jakoby, W. B., ed.) Vol. 22, Academic Press, New York, pp. 565-578.
12. Weber, K., and Osborne, M. (1969) *J. Biol. Chem.*, **244**, 4406-4412.
13. Gelotte, B. (1960) *J. Chromatogr.*, **3**, 330-342.
14. Bradford, M. M. (1976) *Anal. Biochem.*, **72**, 248-254.
15. Rose, T. M., Henikoff, J. G., and Henikoff, S. (2003) *Nucleic Acids Res.*, **31**, 3763-3766.
16. Frohman, M. A. (1993) *Meth. Enzymol.*, **218**, 340-356.
17. Veljanovski, V., Vanderbeld, B., Knowles, V. L., Snedden, W. A., and Plaxton, W. C. (2006) *Plant Physiol.*, **142**, 1282-1293.